Dynamics of Charge Transfer and Recombination in a Covalently-Linked, Face-to-Face Electron Donor–Acceptor Complex

Andrew C. Benniston and Anthony Harriman*

Contribution from the Center for Fast Kinetics Research, The University of Texas at Austin, Austin, Texas 78712

Received May 25, 1994[⊗]

Abstract: The photophysical properties of a covalently-linked, electron donor–acceptor (EDA) complex, containing 1,4-dialkoxybenzene and *N,N'*-dialkyl-4,4'-bipyridinium dication subunits, have been studied in polar solvents. The structure of the compound has been elucidated by X-ray crystallography, 2D NMR, and resonance Raman spectroscopy. Excitation of the ground-state EDA complex with a short laser pulse results in formation of the corresponding excited charge-transfer state, which is weakly fluorescent. The excited state decays, at least in part, via charge transfer to form an intimate radical ion pair (RIP) within a few picoseconds. The free energy content of the RIP decreases with increasing polarity of the solvent, and there is a concomitant increase in the rate of charge recombination, which also occurs on the picosecond time scale. For this system, the dynamics for deactivation of the RIP can be described satisfactorily in terms of both conventional nonadiabatic electron-transfer theory and an exponential energy gap law.

Excitation of an intimate electron donor–acceptor (EDA) complex at a wavelength corresponding to a charge-transfer absorption transition results in formation of an excited charge-transfer state, which may relax to a different orientation from that of the ground state.[1] The excited state can often be detected by transient absorption spectroscopy,[2] enabling the rate of deactivation to be determined, and, usually only in a nonpolar solvent, by luminescence spectroscopy.[3] In competition with restoration of the ground-state EDA complex the excited state may undergo further charge transfer to form an intimate radical ion pair (RIP).[1] The rate of this latter process may be enhanced by polar solvents[2] while formation of the RIP may involve a substantial change in orientation of the reacting species.[4] The lifetime of the excited charge-transfer state,[2] the magnitude of the geometry change,[5] and the lifetime of the RIP[6,7] have been shown to depend markedly on the nature of the reactants. Furthermore, for long-lived RIPs additional geometry changes can take place which allow a solvent molecule to become inserted between the radical ions,[8] forming a solvent-separated RIP. This latter species may dissociate to solvated radical ions or undergo charge recombination to reform the ground-state EDA complex.[1]

Many different types of EDA complexes have been investigated, and much is now known about the dynamics of charge recombination (CR) in solvent-separated RIPs[9] and in certain intimate RIPs formed by ion pairing via electrostatic attractive forces.[10–12] Less success has been achieved with weakly-associated van der Waals complexes,[13] partly because of structural uncertainties and large-scale geometry changes that can take place subsequent to excitation. However, we have recently shown that RIPs can be formed by laser excitation of EDA complexes generated by incarceration of an electron donor into the central cavity of an electron-deficient cyclophane.[14] The main attraction of these particular systems concerns the well-defined ground-state structures and the relatively high association constants. In attempting to better understand the dynamics of CR in such cyclophane-derived EDA complexes, we have studied the corresponding processes occurring in an EDA complex formed by covalent tethering of the same reactants in an approximate face-to-face configuration. Somewhat similar EDA complexes have been studied by Verhoeven and co-workers[15] who described orbital symmetry effects on their absorption and emission spectral properties. Long-lived emission was observed for certain complexes in nonpolar media

[⊗] Abstract published in *Advance ACS Abstracts*, November 15, 1994.

(1) Foster, R. *Organic Charge-Transfer Complexes*: Academic Press: New York, 1969.

(2) Asahi, T.; Ohkohchi, M.; Mataga, N. *J. Phys. Chem.* **1993**, *97*, 13132.

(3) Gould, I. R.; Noukakis, D.; Gomez-Jahn, L.; Young, R. H.; Goodman, J. L.; Farid, S. *Chem. Phys.* **1993**, *176*, 439.

(4) Asahi, T.; Mataga, N. *J. Phys. Chem.* **1991**, *95*, 1956.

(5) Ojima, S.; Miyasaka, H.; Mataga, N. *J. Phys. Chem.* **1990**, *94*, 4147.

(6) (a) Mataga, N.; Shioyama, H.; Kanda, Y. *J. Phys. Chem.* **1987**, *91*, 314. (b) Mataga, N.; Kanda, Y.; Asahi, T.; Miyasaka, H.; Okada, T.; Kakitani, T. *Chem. Phys.* **1988**, *127*, 239. (c) Asahi, T.; Mataga, N. *J. Phys. Chem.* **1989**, *93*, 6575. (d) Miyasaka, H.; Ojima, S.; Mataga, N. *J. Phys. Chem.* **1989**, *93*, 3380. (e) Mataga, N.; Nishikawa, S.; Asahi, T.; Okada, T. *J. Phys. Chem.* **1990**, *94*, 1443.

(7) (a) Hubig, S. M.; *J. Phys. Chem.* **1992**, *96*, 2903. (b) Yabe, T.; Kochi, J. K. *J. Am. Chem. Soc.* **1992**, *114*, 4491. (c) Thompson, P. A.; Simon, J. D. *J. Am. Chem. Soc.* **1993**, *115*, 5657. (d) Sakurai, T.; Yokono, M.; Komiya, K.; Masuda, Y.; Inoue, H. *J. Chem. Soc., Chem. Commun.* **1993**, 1689.

(8) Peters, K. S.; Li, B. *J. Phys. Chem.* **1994**, *98*, 401 and references therein.

(9) (a) Ohno, T.; Yoshimura, A.; Mataga, N. *J. Phys. Chem.* **1986**, *90*, 3295. (b) Ohno, T.; Yoshimura, A.; Mataga, N.; Tazuke, S.; Kawanishi, Y.; Kitamura, N. *J. Phys. Chem.* **1989**, *93*, 3546. (c) Gould, I. R.; Moser, J. E.; Ege, D.; Farid, S. *J. Am. Chem. Soc.* **1988**, *110*, 1991. (d) Gould, I. R.; Moody, R.; Farid, S. *J. Am. Chem. Soc.* **1988**, *110*, 7242. (e) Gould, I. R.; Ege, D.; Moser, J. E.; Farid, S. *J. Am. Chem. Soc.* **1990**, *112*, 4290. (f) Gould, I. R.; Young, R. H.; Moody, R. E.; Farid, S. *J. Phys. Chem.* **1991**, *95*, 2068. (g) Gould, I. R.; Farid, S. *J. Am. Chem. Soc.* **1993**, *115*, 4814.

(10) Segawa, H.; Takehara, C.; Honda, K.; Shimidzu, T.; Asahi, T.; Mataga, N. *J. Phys. Chem.* 1992, *96*, 503.

(11) Zou, C.; Miers, J. B.; Ballew, R. M.; Dlott, D. D.; Schuster, G. B. *J. Am. Chem. Soc.* **1991**, *113*, 7823.

(12) Brun, A. M.; Harriman, A.; Hubig, S. M. *J. Phys. Chem.* **1992**, *96*, 254.

(13) Tachiya, M.; Murata, S. *J. Am. Chem. Soc.* **1994**, *116*, 2434.

(14) Benniston, A. C.; Harriman, A.; Philp, D.; Stoddart, J. F. *J. Am. Chem. Soc.* **1993**, *115*, 5298.

(15) (a) Schroff, L. G.; van der Weerdt, A. J. A.; Staalman, D. J. H.; Verhoeven, J. W.; de Boer, Th. J. *Tetrahedron Lett.* **1973**, 1649. (b) Borkent, J. H.; Verhoeven, J. W.; de Boer, Th. J. *Chem. Phys. Lett.* **1976**, *42*, 50. (c) Zsom, R. L. J.; Schroff, L. G.; Bakker, C. J.; Verhoeven, J. W.; Wright, J.

0002-7863/94/1516-11531$04.50/0

Scheme 1

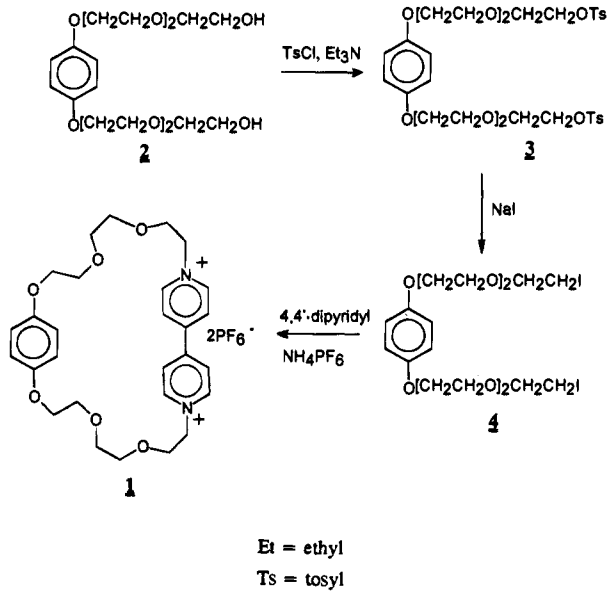

while discrete intramolecular charge-transfer absorption bands were evident in all cases.[15] Our present EDA system, which differs from the many studied by Verhoeven *et al.* by virtue of possessing different redox active subunits and by the existence of strong Coulombic repulsion within the RIP, displays both charge-transfer absorption and emission bands in polar solvents at ambient temperature. This facilitates a more complete evaluation of the photophysical properties of the system.

Experimental Section

The cyclophane **1** was prepared according to Scheme 1. Compound **2** was synthesized by standard methods and subsequently converted into the diiodide **4** via two successive steps. Cyclization was carried out using high-dilution techniques in which **4** (7.0 g, 11.2 mmol) was dissolved in dried CH_3CN (500 mL) and brought to a gentle reflux under vigorous stirring. 4,4′-Bipyridyl (1.75 g, 11.2 mmol) in dried CH_3CN (150 mL) was added over a period of 6 h, and the solution was stirred for a further 48 h before being cooled and filtered. The solvent was removed under vacuum to give a dark red oil which was stirred with water (150 mL). The aqueous layer was separated, filtered, and treated with an excess of a saturated aqueous solution of NH_4PF_6. The resultant dark red precipitate was collected, slurried with CH_3OH, and dried under vacuum. Yield: 1.63 g, 19%. ^1H NMR (acetone-d_6): δ = 3.73−3.86 (m, 14H); 4.13−4.16 (m, 6H); 5.08−5.11 (t, 4H, J = 4.7 Hz); 6.85 (s, 4H); 8.15−8.18 (d, 4H, J = 6.9 Hz); 9.30−9.33 (d, 4H, J =6.9 Hz). ^{13}C NMR (acetone-d_6): δ = 62.2 (2C); 68.8 (2C); 69.3 (2C); 70.2 (2C); 70.5 (2C); 70.8 (2C); 116.4 (4C); 127.0 (4C); 147.4 (4C); 150.5 (2C); 153.9 (2C). FAB MS (nitrobenzyl alcohol matrix): m/z 786 $\{[M(PF_6)_2]^+\}$; 641 $\{[M - PF_6]^+\}$; 496 $\{[M - H]^+\}$. Anal. Calcd for $C_{28}H_{36}N_2O_6P_2F_6$: C, 42.96; H, 4.61; N, 3.56. Found: C, 42.99; H, 4.66; N, 3.38. Crystals suitable for X-ray diffraction were grown by vapor diffusion of ether into a solution of **1** in acetone. The atomic coordinates, bond angles and distances, and crystal parameters are provided in the supplementary material. All solvents used for spectroscopic studies were spectral grade materials and were checked for fluorescent impurities.

^1H NMR spectra were recorded with a Bruker AC250 instrument with TMS as the internal reference. Rotating frame nuclear Overhauser effect (ROE) spectroscopy was done with a Bruker AX500 instrument. Absorption spectra were recorded with a Hitachi U3210 spectrophotometer, and fluorescence spectra were recorded with a fully-corrected Perkin-Elmer LS5 spectrofluorimeter. Fluorescence lifetimes were measured by time-correlated, single-photon counting using a synchronously-pumped, cavity-dumped, mode-locked Styryl-9 dye laser. Excitation was made at 410 nm, and emission was collected at six discrete wavelengths and analyzed by global analysis methodology. Fluorescence was isolated from scattered laser light using a high-radiance monochromater and was detected with a Hamamatsu R2809U microchannel plate phototube. After deconvolution of the instrument response function, the ultimate temporal resolution of this setup was *ca.* 15 ps. Solutions were adjusted to possess an absorbance at 400 nm of *ca.* 0.10 and were deoxygenated with N_2.

Transient absorption spectral measurements were made with a purpose-built Styryl-9 dual-jet dye laser synchronously pumped at 76 MHz by the frequency-doubled output of a cw mode-locked Nd:YAG laser (Coherent Antares 76S). The dye laser output was directed through a three-stage dye amplifier (Quantel PTA-60) pumped at 10 Hz by the frequency-doubled output of a regeneratively amplified Nd:YAG laser (Continuum RGA-67-10). Amplification gave output pulses of *ca.* 1 mJ at 800 nm having a fwhm (full width at half-maximum) of *ca.* 350 fs. The excitation pulse was frequency doubled and directed almost collinearly with the analyzing white light continuum pulse through the sample cell; the latter was generated by focusing residual excitation into water. Approximately 500 individual laser pulses were collected at each delay time and averaged in a microcomputer. Transient absorption spectra were compiled by subtracting successive pulses with and without excitation while kinetic profiles were generated by overlaying spectra collected at about 30 different delay times. Analysis was made by nonlinear, least-squares computer iteration using global analysis methodology. Solutions for laser flash photolysis were adjusted to possess an absorbance of *ca.* 0.4 at 400 nm and were deoxygenated with N_2.

Electrochemical redox potentials were determined by cyclic voltammetry for **1** in dried CH_3CN solution (1.5 mM) containing tetra-*N*-butylammonium perchlorate (0.2 M). A glassy carbon working electrode was used in conjunction with a Pt counter electrode and an SCE reference. Solutions were purged thoroughly with N_2 prior to electrolysis. The redox potential for one-electron oxidation of the dialkoxybenzene subunit in **1** was determined to be 1.38 ± 0.06 V vs SCE while the redox potential for one-electron reduction of the *N,N*′-dialkyl-4,4′-bipyridinium subunit in **1** was found to be -0.48 ± 0.05 V vs SCE. Assignment of individual electrode processes was made by reference to 1,4-dimethoxybenzene and *N,N*′-dimethyl-4,4′-bipyridinium bis(hexafluorophosphate). Identical studies were made with **1** dissolved in other polar solvents, and the results are discussed in the text.

Resonance Raman studies were carried out in CH_3CN solution using an argon ion laser as the excitation source. The solution was contained in a capillary tube and illuminated at 514.5 nm. Scattered Raman signals were collected with a Cassegrain lens and dispersed with a Spex 1877 Triplemate monochromater before being detected with a dual diode array spectrograph.

Results

Structural Features. In the solid state, **1** possess a slightly distorted face-to-face configuration as shown by the X-ray crystallographic structure exhibited in Figure 1. The 4,4′-bipyridinium dication is nonplanar, although the individual rings are planar, with a dihedral angle between the two pyridinium rings of 23.0°. One of these rings lies almost parallel to the phenyl ring of the dialkoxybenzene subunit, having a dihedral angle of only 3.9°. The interplanar distance between the center of the phenyl ring and the 4,4′-bipyridinium subunit is 3.42 Å although the 4,4′-bipyridinium dication is slightly twisted with respect to the phenyl ring (Figure 1a). The twist angle of 33.4° is comparable to those observed for related cyclophane-derived EDA complexes.[16] This structural information indicates that,

D.; Kuroda, H. *Tetrahedron* **1978**, *34*, 3225. (d) Verhoeven, J. W.; Kroon, J.; Paddon-Row, M. N.; Warman, J. M. In *Supramolecular Chemistry*; Balzani, V., De Cola, L., Eds.; NATO ASI Series C; Kluwer: Dordrecht, Vol. 371, 1992; The Netherlands, p 181.

(16) Anelli, P. L.; Ashton, P. R.; Ballardini, R.; Balzani, V.; Delgado, M.; Gandolfi, M. T.; Goodnow, T. T.; Kaifer, A. E.; Philp, D.; Pietraszkiewicz, M.; Prodi, L.; Reddington, M. V.; Slawin, A. M. Z.; Spencer, N.; Stoddart, J. F.; Vicent, C.; Williams, D. J. *J. Am. Chem. Soc.* **1992**, *114*, 193.

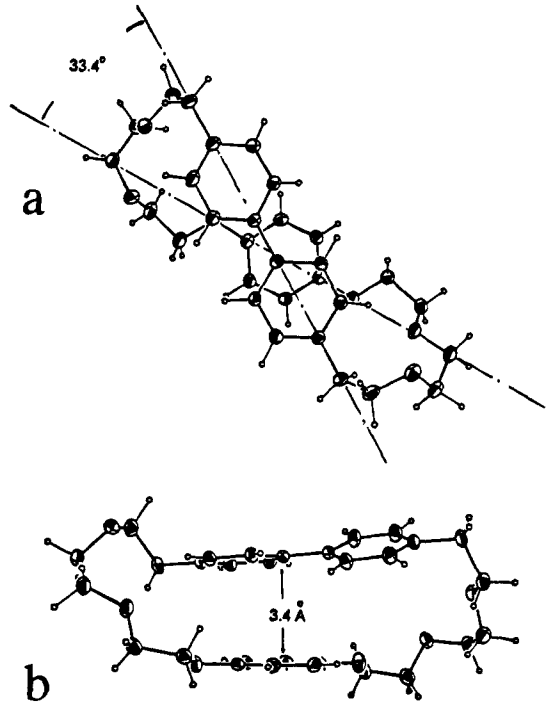

Figure 1. X-ray crystal structure for **1** showing (a) the view from above and (b) the view from the side. The parameters are given in the supplementary material.

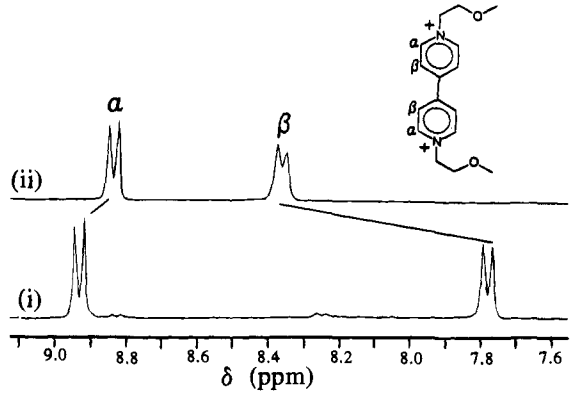

Figure 2. Partial ^{1}H NMR spectra recorded for (i) **1** and (ii) *N,N'*-dimethyl-4,4'-bipyridinium bis(hexafluorophosphate) in CD_3CN solution.

in the solid state, the redox-active subunits are in van der Waals contact (Figure 1b).

Solution phase ^{1}H NMR spectral measurements are also consistent with intimate contact between the dialkoxybenzene ring and the 4,4'-bipyridinium dication. Thus, in CD_3CN solution significant shifts are observed for both the α- and β-protons on the 4,4'-bipyridinium dication (Figure 2). The α-protons are shifted downfield by 0.11 ppm while the β-protons undergo an upfield shift of 0.58 ppm relative to *N,N'*-dimethyl-4,4'-bipyridinium bis(hexafluorophosphate) in CD_3CN. A similar effect was observed for the corresponding 4,4'-bipyridinium dication subunits in cyclophane-derived catenates[16] and pseudorotaxanes,[17] where it was attributed to the close proximity of donor and acceptor π-electron clouds. In fact, the close intimacy of donor and acceptor subunits in **1** was confirmed unequivocally by 2D ROE experiments made in acetone-d_6 (Figure 3). Both the CH(α) and CH(β) protons on the *N,N'*-bipyridinium dication show cross-peaks to protons on the

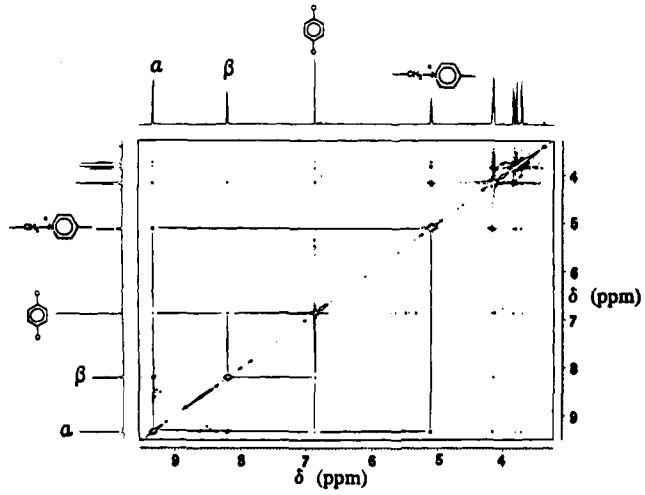

Figure 3. 2D ROE ^{1}H NMR spectrum recorded for **1** in acetone-d_6.

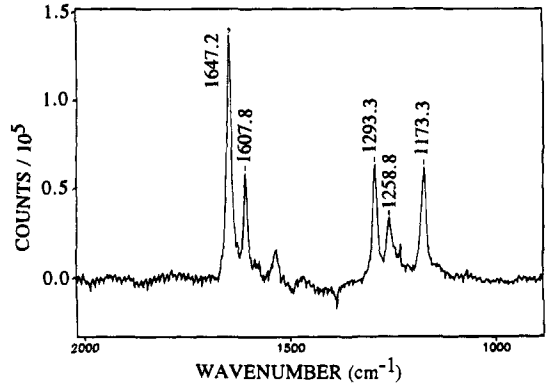

Figure 4. Resonance Raman spectrum recorded for **1** in CH_3CN solution.

Table 1. Resonance Raman Spectral Data Derived for **1** in Acetonitrile Solution

ν_i/cm^{-1}	I_{rel}	Δ	λ_i/cm^{-1}	assignment
1173.4	1.00	0.45	119	CCH in plane
1258.9	0.67	0.39	96	C=C interring
1293.3	1.12	0.44	125	C=N ring stretch
1525.0	0.40	0.31	73	ring stretch
1607.8	1.02	0.38	116	C=C ring stretch
1647.9	2.37	0.47	182	C=N ring stretch

dialkoxybenzene subunit. This finding indicates that the subunits must lie within 4 Å of each other, at least for several hundred milliseconds. As expected, NOE effects between the CH(α) and CH(β) protons and the CH_2 protons of the polyethoxy chain are clearly apparent. It appears, therefore, that the redox-active subunits in **1** remain closely-coupled in both the solution and solid phases; examination of space-filling molecular models indicates that the maximum separation of the π-clouds is only *ca.* 5.6 Å. Although the EDA complex possesses considerable degrees of orientational freedom, it appears unlikely that a solvent molecule can penetrate between the reactants, before or after irradiation.

Resonance Raman Spectroscopy. We have collected resonance Raman spectral data for **1** in CH_3CN solution (Figure 4), and the major vibrational modes (ν_i), together with their assignment and normalized scattering intensity (I_{rel}), are collected in Table 1. Following the procedures reported by Doorn *et al.*,[18] the displacement parameters (Δ) and vibrational

(17) Ashton, P. R.; Philp, D.; Spencer, N.; Stoddart, J. F.; Williams, D. J. *J. Chem. Soc., Chem. Commun.* **1994**, 181.

(18) Doorn, S. K.; Blackbourn, R. L.; Johnson, C. S.; Hupp, J. T. *Electrochim. Acta* **1991**, *36*, 1775.

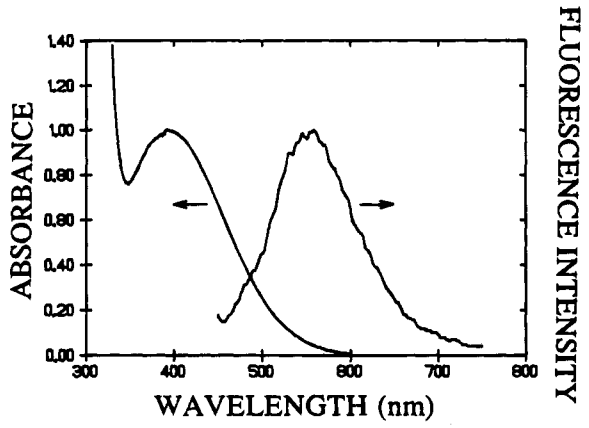

Figure 5. Absorption and fluorescence spectra recorded for **1** in CH_3CN solution.

reorganization energies (λ_i) for individual modes were calculated (Table 1). Summation of the individual reorganization energies gives a total vibrational reorganization energy (λ_{vib}) of *ca.* 710 cm^{-1} (i.e., *ca.* 0.09 eV). The six major Raman-active modes can be averaged to give a single representative vibrational frequency (ν_q) of 1445 cm^{-1} using the following expression:[18]

$$\nu_q = [\sum \nu_i^2 \lambda_i / \lambda_{vib}]^{1/2} \quad (1)$$

The relatively low value found for λ_{vib} suggests to us that there is only a modest structural change accompanying excitation of the ground-state EDA complex. This might indicate that the (relaxed) excited charge-transfer state and the ground-state EDA complex possess similar geometries. The major orientational change expected for the excited state, assuming this species possesses more charge-transfer character than does the ground state, concerns decreasing the dihedral angle between the two pyridinium rings. Increasing the amount of charge-transfer character will also result in increased Coulombic repulsion between the redox-active subunits, and this might induce spatial separation of the subunits. Of course, the connecting chains prevent substantial geometry changes, and it is interesting to note that the derived λ_{vib} is approximately 25% of that observed for a weakly-bound, intermolecular EDA complex.[19]

Absorption and Emission Spectroscopy. Absorption spectra recorded for **1** in CH_3CN solution exhibit a Gaussian-shaped band centered around 397 nm, with a molar extinction coefficient (ϵ) of 130 M^{-1} cm^{-1} (Figure 5), which is absent from spectra recorded for the individual components. This band, which displayed a half-width ($\Delta\nu_{1/2}$) of 6800 cm^{-1}, is assigned to a charge-transfer transition within the confines of an EDA complex in which electronic charge is transferred from the dialkoxybenzene subunit to the 4,4′-bipyridinium dication.[14] A similar spectrum is obtained by treating 1,4-dimethoxybenzene with excess *N,N′*-dimethyl-4,4′-bipyridinium bis(hexafluorophosphate) in CH_3CN, or *vice versa*, although here the band maximum occurs at 406 nm (ϵ = 670 M^{-1} cm^{-1}) and the association constant ($K \approx 0.5$ M^{-1}) is very low. Excitation of **1** in CH_3CN at 400 nm gives rise to an extremely weak emission band, centered at 520 nm (Figure 5); the emission quantum yield was too low for accurate determination. The corrected excitation spectrum showed reasonably good correspondence with the charge-transfer absorption band, considering that large slit widths had to be used to properly resolve the emission band. Emission is attributed to radiative deactivation of the excited charge-transfer state, and has been reported previously for both intermolecular[20] and intramolecular[21] EDA complexes in nonpolar solvents. Time-resolved fluorescence spectroscopy indicated that the lifetime of the excited charge-transfer state was less than 15 ps since emission could not be satisfactorily resolved from the instrumental response.

Table 2. Absorption and Emission Spectral Parameters Derived for **1** in a Series of Polar Solvents

solvent	ν_{abs}/cm^{-1}	ν_{ems}/cm^{-1}	V/cm^{-1}	λ/eV	E_{es}/eV
CH_3CN	19 175	25 075	900	0.37	2.74
$(CH_3)_2SO$	19 220	24 555	860	0.33	2.71
C_4H_9CN	19 400	24 810	920	0.33	2.74
PC[a]	18 810	24 905	900	0.38	2.71
$HCONH_2$	19 190	24 795	900	0.35	2.73
$(CH_3)_2CO$	18 525	24 400	890	0.36	2.66
$HCON(CH_3)_2$	19 620	24 955	860	0.33	2.76
CH_3NO_2	18 990	24 960	880	0.37	2.72

[a] PC = propylene carbonate.

The observed charge-transfer absorption and emission bands were analyzed in terms of a Gaussian-shaped profile in order to derive energies for the band maxima. The absorption (ν_{abs}) and emission (ν_{ems}) maxima so obtained are given in Table 2 and were used to calculate the energy level for the excited state (E_{es}) and the total reorganization energy (λ) that accompanies its formation.

$$E_{es} = (hc/2)[\nu_{abs} + \nu_{ems}] \quad (2)$$

$$\lambda = (hc/2)[\nu_{abs} - \nu_{ems}] \quad (3)$$

The derived energy level (E_{es} = 2.74 ± 0.02 eV) can be compared with the redox potential difference observed for **1** (ΔE° = 1.86 ± 0.11 eV), without correction for Coulombic work terms. The total reorganization energy (λ = 0.37 ± 0.03 eV) is normally considered to be the summation of vibrational (λ_{vib} = 0.09 eV) and solvent (λ_{sol}) terms.[22] Consequently, λ_{sol} is expected to be *ca.* 0.28 eV. The absorption spectral data were also used to estimate the degree of electronic coupling between the reactants (V) in the ground-state EDA complex[23]

$$V = \frac{0.0206[\epsilon \nu_{abs} \Delta\nu_{1/2}]^{1/2}}{d} \quad (4)$$

where d is the separation distance (d = 3.4 Å). The derived value for V is 900 cm^{-1} (i.e., 0.11 eV) (Table 2) and indicates strong coupling between the reactants in the ground state. The half-width of the emission band ($\Delta\nu_{1/2} \approx 4000$ cm^{-1}) was significantly less than that of the corresponding absorption band ($\Delta\nu_{1/2} \approx 6800$ cm^{-1}).

Identical spectral measurements, and subsequent calculations, were made for **1** in a range of polar solvents, and the results are compiled in Table 2. It is seen that the nature of the solvent exerts only a minor influence on the spectral profiles and, within experimental limitations, hardly affects the magnitude of the derived parameters. In particular, the energy level for the excited charge-transfer state (E_{es} = 2.72 ± 0.04 eV), total reorganization energy (λ = 0.35 ± 0.04 eV), and electronic coupling matrix element for the ground-state EDA complex (V = 890 ± 30 cm^{-1}) remain almost invariant to the nature of the solvent. For these solvents, there are no obvious effects of ion-pairing under the conditions used. However, the Stokes' shift

(19) Markel, F.; Ferris, N. S.; Gould, I. R.; Myers, A. B. *J. Am. Chem. Soc.* **1992**, *114*, 6208.
(20) (a) Gould, I. R.; Noukakis, D.; Gomez-Jahn, L.; Young, R. H.; Goodman, J. L.; Farid, S. *J. Am. Chem. Soc.* **1993**, *115*, 3830. (b) Gould, I. R.; Young, R. H.; Mueller, L. J.; Albrecht, A. C.; Farid, S. *J. Am. Chem. Soc.* **1994**, *116*, 3147.
(21) *The Exciplex*; Gordon, M., Ware, W. R., Eds.; Academic Press: New York, 1975.
(22) Marcus, R. A. *J. Phys. Chem.* **1989**, *93*, 3078.
(23) Hush, N. S. *Prog. Inorg. Chem.* **1967**, *8*, 391.

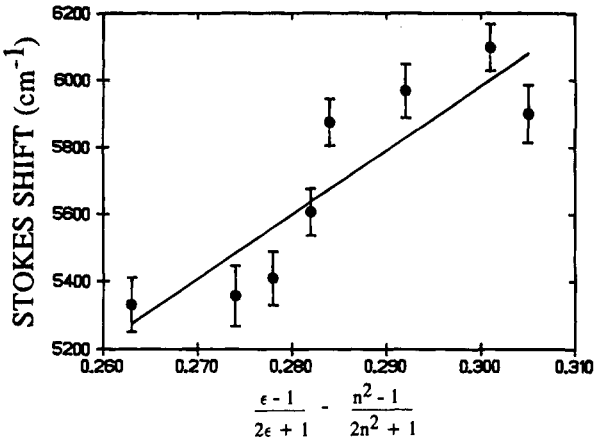

Figure 6. Correlation between the observed Stokes' shift and the reaction field parameter as measured for **1** in a series of polar solvents. For the reaction field parameter, n is the refractive index and ϵ is the static dielectric constant of the solvent.

exhibits a small but clear dependence on the solvent reaction field parameter,[24] as shown in Figure 6, indicating that excitation involves a definite change in dipole moment.

In ideal cases, the solvent reorganization energy can be measured by monitoring the effect of solvent polarity on the absorption band maximum or by monitoring the band half-width as a function of temperature. Such studies were made, but the wide scatter in data points and possible conformational changes render the derived parameters unreliable. Instead, it was assumed that $\lambda_{vib} = 0.09$ eV in all solvents so that λ_{sol} could be estimated from the total reorganization energy obtained from spectral analysis. It can be seen from inspection of the values compiled in Table 2 that λ_{sol} is essentially independent of solvent for the narrow range of solvents used.

Transient Absorption Spectroscopy. Immediately after excitation of **1** in CH_3CN solution with a 350-fs laser pulse at 400 nm a transient absorption spectral profile was observed that resembled the characteristic features of the 4,4′-bipyridinium cation radical (Figure 7a). This transient spectrum is assigned to the excited charge-transfer state formed upon direct excitation of the ground-state EDA complex. Small absorption spectral shifts occur during the first few picoseconds after excitation (Figure 7a), followed by decay of the residual absorbance to the prepulse baseline (Figure 7b,c). These changes are ascribed to conversion of the excited charge-transfer state into an intimate RIP and subsequent CR within the RIP to reform the ground-state EDA complex. Kinetic profiles were nonexponential but could be analyzed in terms of dual-exponential processes. The lifetime of the faster decaying component, believed to be the excited charge-transfer state, was close to the time resolution of the instrument (i.e., ~1 ps), but the lifetime of the longer-lived component (τ_{CR}) could be resolved easily. The computed value in acetonitrile solution was 66 ± 6 ps (Figure 7c). The lifetime of the excited charge-transfer state (τ_f) was derived to be 3.5 ± 1.5 ps (Figure 7b).

Similar transient absorption spectral changes were observed in other polar solvents and were analyzed as above. Kinetic profiles recorded in all solvents required analysis in terms of two-exponential fits, with the longer-lived component having a lifetime (τ_{CR}) significantly longer than that the shorter-lived species (τ_f). In such cases, therefore, the RIP is considered to be much longer lived than the corresponding excited charge-transfer state. For these solvents, the lifetime of both the excited

(24) Khundkar, L. R.; Stiegman, A. E.; Perry, J. W. *J. Phys. Chem.* **1990**, *94*, 1224.

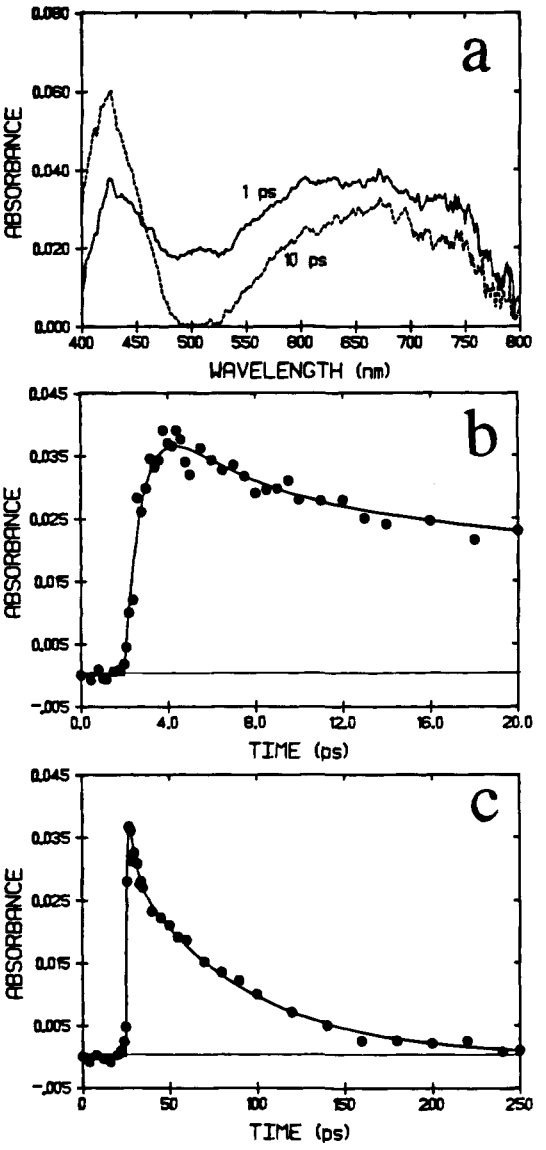

Figure 7. (a) Transient absorption spectra recorded 1 and 10 ps after excitation of **1** in CH_3CN solution with a 350 fs laser pulse at 400 nm. The spectra were corrected for spectral chirp. (b, c) Decay profiles recorded at 600 nm, with the solid line referring to a kinetic fit to the sum of two exponentials having lifetimes of 3.5 and 66 ps.

Table 3. Kinetic and Thermodynamic Parameters Derived for **1** in a Series of Polar Solvents

solvent	$\Delta E°$/eV	$-\Delta G_{CT}°$/eV	$-\Delta G_{CR}°$/eV	ϵ_s	τ_f/ps[b]	τ_{ct}/ps[c]
CH_3CN	1.86	0.59	2.15	37.5	3.5	66
$(CH_3)_2SO$	1.88	0.62	2.09	46.7	1.6	52
C_4H_9CN	1.86	0.42	2.32	23.0	8.5	118
PC[a]	1.86	0.68	2.03	65.3	1.7	50
$HCONH_2$	1.81	0.82	1.91	110	1.2	33
$(CH_3)_2CO$	1.75	0.39	2.27	20.7	7.0	100
$HCON(CH_3)_2$	1.81	0.82	1.91	36.7	1.2	40
CH_3NO_2	1.76	0.69	2.03	38.6	2.0	48

[a] PC = propylene carbonate. [b] ±30%. [c] ±10%.

charge-transfer state and the RIP increased with decreasing polarity of the solvent (Table 3).

Discussion

Our results can be discussed in terms of the free energy diagram depicted in Figure 8, which follows from the prior work of Mataga and co-workers.[2] Excitation of the ground-state EDA

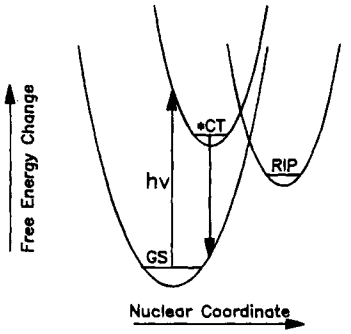

Figure 8. Potential energy level diagram showing excitation of **1** at a wavelength corresponding to the charge-transfer absorption band.

complex at a wavelength corresponding to the charge-transfer absorption band results in population of the excited charge-transfer state. The polarity of this excited state differs somewhat from that of the ground state and, because of increased Coulombic repulsion between the aromatic subunits, the equilibrated conformation differs from that of the ground state, as indicated by the substantial Stokes' shift. Deactivation of the excited charge-transfer state can involve luminescence, internal conversion to the ground state, or charge transfer to form a RIP. The latter process involves an additional nuclear displacement. The energy level of the RIP is expected to decrease with increasing polarity of the surrounding solvent, due to solvent stabilization of the π-radical ions, and there should be a concomitant decrease in the height of the barrier to formation of the RIP with increasing solvent static dielectric constant (ϵ_s). Thus, the lifetime of the excited charge-transfer state is expected to decrease with increasing solvent polarity (Table 3). Identical effects have been investigated thoroughly with intermolecular,[20] intramolecular,[21] and cyclophane-derived[14,15] EDA systems.

The RIP decays rapidly, despite the large amount of energy that must be dissipated during nonradiative deactivation. It is difficult to determine the exact free energy content of the RIP but this value can be approximated as follows:

$$\Delta G_{CR}^{\circ} = -[\Delta E^{\circ} + (e^2/d\epsilon_s)] \qquad (5)$$

where the separation distance d is assumed to be the maximum value of 5.6 Å and ΔE° is the redox potential difference recorded in that particular solvent (Table 3). The derived values are collected in Table 3 and are seen to decrease from −1.91 to −2.32 eV as the solvent dielectric constant decreases from 110 to 21. Deactivation of the RIP involves reformation of the ground-state EDA complex and, therefore, is attributed to CR, for which there might be a significant change in the nuclear coordinates (Figure 8). Figure 9 now shows the relationship between the rate of CR ($k_{CR} = 1/\tau_{CR}$) and the free energy content of the RIP within the narrow range of the free energy change. It is apparent that the rate of CR decreases exponentially with increasing reaction exergonicity, according to

$$k_{CR} = 1/\tau_{CR} = A \exp[-\delta \Delta G_{CR}^{\circ}] \qquad (6)$$

where $A \approx 1 \times 10^{13}$ s^{-1} and $\delta = 3.1 \pm 0.2$ eV^{-1}. This situation is reminescent of the energy gap law describing nonradiative deactivation of excited states[25] and has been observed previously for CR within certain intimate RIPs.[13] Thus, Mataga and coworkers have observed similar behavior for electrostatically-bound metalloporphyrins ($\delta = 5.5$ eV^{-1})[10] and strongly-coupled EDA complexes ($\delta = 3.2$ eV^{-1})[2] while we have observed

(25) Freed, K. M.; Jortner, J. *J. Chem. Phys.* **1970**, *52*, 6272.

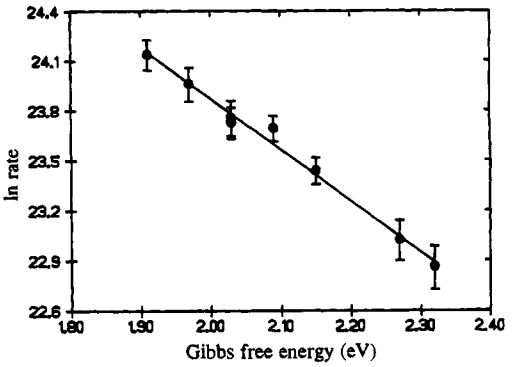

Figure 9. Effect of reaction exergonicity on the rates of CR as measured for **1** in a series of polar solvents. The solid line drawn through the data points corresponds to a least-squares fit to eq 6 with the parameters given in the text.

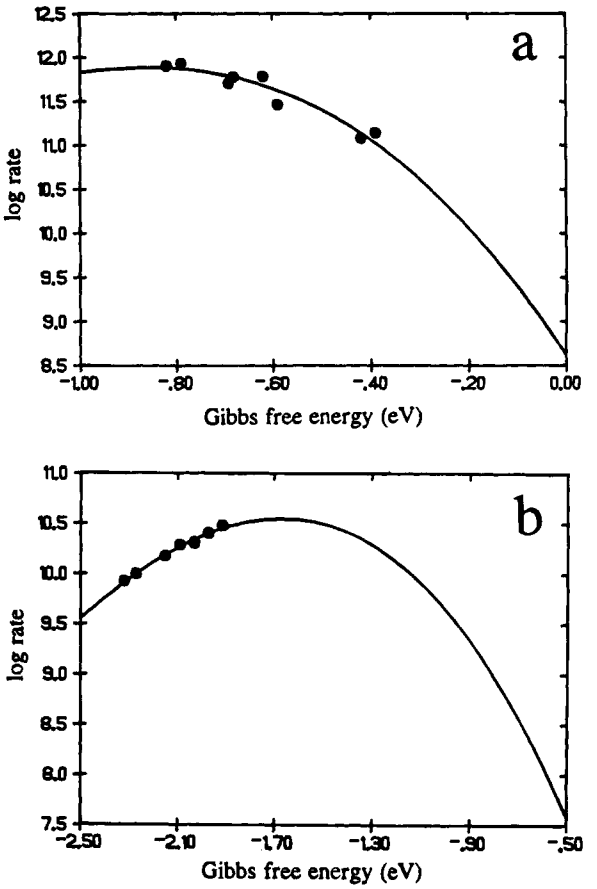

Figure 10. Effect of reaction exergonicity on the rates of (a) charge transfer and (b) charge recombination as measured for **1** in a series of polar solvents. The solid curve drawn through the data points corresponds to the best fit to the Jortner–Rips expression with the parameters given in the text.

comparable properties for both highly-charged complexes ($\delta = 3.4$ eV^{-1})[12,26] and cyclophane-derived RIPs ($\delta = 1.75$ eV^{-1}).[14] Such an energy gap relationship would arise if there is a high density of vibrational states in the vicinity of ΔG_{CR}° while a low value for δ indicates a high electronic–vibronic coupling constant.[27]

At this point it is instructive to consider if the rates of electron transfer can be accommodated in terms of conventional electron-transfer theory.[28] Unfortunately, neither the magnitude of the electronic coupling matrix element (V) nor the total reorganiza-

(26) Brun, A. M.; Harriman, A. *J. Am. Chem. Soc.* **1991**, *113*, 8153.
(27) Caspar, J. V.; Meyer, T. J. *J. Phys. Chem.* **1983**, *87*, 952.

tion energy (λ) can be extracted from spectroscopic data. It is likely, however, that electronic coupling within the RIP will be much weaker than that in the ground-state EDA complex, because of the increased Coulombic repulsion and that CR will be under nonadiabatic control. For formation of the RIP from the excited charge-transfer state, the reaction exergonicity can be estimated as

$$\Delta G_{CT}^{\circ} = -[E_{es} + \Delta G_{CR}^{\circ}] \quad (7)$$

and the derived values are compiled in Table 3. There is only a small variation in ΔG_{CT}°, because of the restricted choice of solvent, but, as can be seen from Figure 10a, there is a smooth correlation between the rate of charge transfer ($k_{CT} \approx 1/\tau_f$) and ΔG_{CT}°. The curve drawn through the data points in Figure 10a corresponds to a fit to the Jortner–Rips expression for nonadiabatic electron transfer between weakly-coupled reactants[28] with $V = 60$ cm^{-1}, $\nu = 1445$ cm^{-1}, $\lambda_{vib} = 0.2$ eV, and $\lambda_{sol} = 0.70$ eV. Because of the limited range of ΔG_{CT}° values, these are not unique solutions, but they appear to be quite reasonable. Thus, the magnitude of electronic coupling is modest, the small λ_{vib} value reflects the limited amount of nuclear displacement associated with charge transfer, and the λ_{sol} relates to solvent rearrangement around the highly-charged RIP.

The same expression can be used to fit the data describing CR within the RIP (Figure 10b). Again, there is a very restricted range of ΔG_{CR}° values, ensuring an easy fit! Using $\nu = 1445$ cm^{-1} and $\lambda_{vib} = 0.3$ eV, the best computed fit to the Jortner–Rips expression[28] (Figure 10b) requires that $V = 14$ cm^{-1} and $\lambda_{sol} = 1.38$ eV. While the magnitude of the electronic coupling matrix element seems to be reasonable, the calculated solvent reorganization energy appears somewhat high. However, these are nonunique solutions, and an equally good fit to the experimental data can be achieved with, for example, $V = 16$ cm^{-1}, $\nu = 800$ cm^{-1}, $\lambda_{vib} = 0.3$ eV, and $\lambda_{sol} = 1.02$ eV.

Clearly, the rates of CR for this system can be quantitatively explained either in terms of a simple energy-gap law[2] or *via* conventional nonadiabatic electron-transfer theory.[28] This situation may arise because of the relatively weak coupling between the reactive subunits, due to electrostatic repulsion, or because of the narrow range of reaction exergonicity that is accessible. Other researchers[13,29–31] have tried to rationalize the two theories into a single framework, but there is growing experimental evidence[2,10,12,14,26] that rates of CR within intimate RIPs do not follow normal "bell-shaped" energy-gap profiles. The present study does not help resolve this issue but does provide a comprehensive account of the photophysical properties of intimate EDA complexes. It is interesting to note the progressive decrease in electronic coupling between the redox-active subunits on passing from the ground state ($V = 890$ cm^{-1}) to excited charge-transfer state ($V \approx 60$ cm^{-1}) to RIP ($V \approx 14$ cm^{-1}). This progression is associated with increasing extents of electrostatic repulsion and increasing nuclear displacement. Related studies with cyclophane-derived EDA complexes, where coupling between the reagents is more pronounced than in **1** and where nuclear displacement is less significant, are underway and will be described elsewhere.

Acknowledgment. We thank the NIH (Grant GM48150) for financial support of this work and Dr. V. M. Lynch for recording the X-ray crystallography data. The Center for Fast Kinetics Research is supported by The University of Texas at Austin.

Supplementary Material Available: Text giving an X-ray experimental summary, tables giving positional and isotropic thermal parameters, anisotropic thermal parameters, bond lengths and angles, and torsion angles for **1**, and figures showing the atom labeling scheme of $(C_{32}H_{44}N_2O_6)^{2+}$ and a unit cell packing diagram (16 pages); tables listing observed and calculated structure factor amplitudes for **1** (35 pages). This material is contained in many libraries on microfiche, immediately follows this article in the microfilm version of the journal, and can be ordered from the ACS; see any current masthead page for ordering information.

(28) Rips, I.; Jortner, J. *J. Chem. Phys.* **1987**, *87*, 2090 and references therein.

(29) Gould, I. R.; Noukakis, D.; Gomez-Jahn, L.; Goodman, J. L.; Farid, S. *J. Am. Chem. Soc.* **1993**, *115*, 4405.

(30) Wynne, K.; Galli, C.; Hochstrasser, R. M. *J. Chem. Phys.* **1994**, *100*, 4797.

(31) (a) Walker, G. C.; Barbara, P. F.; Doorn, S. K.; Dong, Y.; Hupp, J. T. *J. Phys. Chem.* **1991**, *95*, 5712. (b) Åkesson, E.; Walker, G. C.; Barbara, P. F. *J. Chem. Phys.* **1991**, *95*, 4188. (c) Walker, G. C.; Åkesson, E.; Johnson, A. E.; Levinger, N. E.; Barbara, P. F. *J. Phys. Chem.* **1992**, *96*, 3728. (d) Kliner, D. A. V.; Tominaga, K.; Walker, G. C.; Barbara, P. F. *J. Am. Chem. Soc.* **1992**, *114*, 8323.